Non-monotonic behaviour of the energy levels of quantum wells with a large mass mismatch in the presence of an in-plane magnetic field

1999 J. Phys.: Condens. Matter 11 6207

(http://iopscience.iop.org/0953-8984/11/32/312)

J. Phys.: Condens. Matter **11** (1999) 6207–6216. Printed in the UK PII: S0953-8984(99)99781-3

Non-monotonic behaviour of the energy levels of quantum wells with a large mass mismatch in the presence of an in-plane magnetic field

R H J De Meester and F M Peeters

Department Natuurkunde, Universiteit Antwerpen (UIA), Universiteitsplein 1, B-2610 Antwerpen, Belgium

E-mail: roeldm@uia.ua.ac.be and peeters@uia.ua.ac.be

Received 30 November 1998, in final form 29 June 1999

Abstract. We present a theoretical study of the electron states in a quantum well with finite barrier height in a magnetic field applied parallel to the quantum well. For large electron mass mismatch between the quantum well and the barrier, we found the surprising result that the electron energy for zero wave vector decreases with decreasing well width and the energy spectrum has a local minimum at a non-zero wave vector. The influence of well depth, mass ratio and magnetic field are investigated.

1. Introduction

Electrons confined by a square well (taken in the z-direction) form a quasi-two-dimensional electron gas. When subjected to an in-plane magnetic field $\vec{B} = B_y \vec{e}_y$ the electrons moving in the x-direction are decelerated or accelerated by the combined effect of the crossed fields B_y and $E_z = -\mathrm{d}V_{conf}(z)/\mathrm{d}z$, while the electron motion in the y-direction is not altered. A great deal of theoretical work has already been done on such systems [1–8], but up to now the mass mismatch between electrons in the well and the barrier was neglected or taken to be relatively small.

It is well known that the mass ratio of charge carriers between the barrier (m_b) and quantum well (m_w) mass has an influence on the bottom of the energy spectrum $E(k_x)$ in the quantum well. In reference [9] Bastard found that this energy decreases with increasing mass ratio $\mu = m_w/m_b$ for fixed quantum well width. Increasing the mass ratio leads to a decreasing penetration of the envelope function into the barrier. Consequently, the modulus of the derivative of the wave function at the edges inside the well becomes smaller and smaller to comply with continuity of $m^{-1}(z)\, \partial\psi/\partial z$ at the interface. Consequently, in the limit of an infinite mass ratio the only possible wave function for the ground state is constant in the well and zero in the barrier and thus the energy of the ground state E_0 becomes zero.

Here we find another effect which is very surprising (in fact it is counter-intuitive) but is related to the observation of Bastard: for a sufficiently large mass ratio, $E_n(k_x = 0)$ decreases with decreasing quantum well width if the well is not too narrow and this decrease is more pronounced with decreasing height of the potential barrier, increasing magnetic field and increasing mass ratio. A consequence of this effect is that the energy spectrum of charge

0953-8984/99/326207+10$30.00

carriers in parallel magnetic fields exhibits a local minimum at $k_x \neq 0$. Previously, local minima in the energy spectrum for $k \neq 0$ were found but they all arise from other causes.

It is known that the spin–orbit interaction present in the Hamiltonian will also lead to such a minimum in the dispersion curve at finite momentum [10] but since this effect is a function of the total magnetic field it can be distinguished from our effect by tilting the magnetic field out of the plane. The present effect would then decrease while the spin–orbit effect would be independent of the tilt angle.

Smrčka and Jungwirth [3] investigated the single-layer/bilayer transition of electrons in AlGaAs/GaAs/AlGaAs wells subject to an in-plane magnetic field. This system is doped which leads to bending of the potential by electronic forces and the system can no longer be described by a square well. Instead there is a soft built-in barrier formed which has approximately an inverted parabolic shape. Self-consistent calculations led them to the observation of a local minimum in $E_n(k)$ at $k \neq 0$ which is the result of the non-square well used, and not of the mass mismatch since this effect has been totally neglected.

Ibrahim and Peeters [11] investigated two-dimensional electrons in lateral magnetic superlattices. Their system is one in which a ferromagnetic film is deposited on a heterostructure and patterned such that the magnetic domains consist of parallel strips with the magnetization perpendicular to the thin film and which changes sign from one strip to the next. They used several different models to describe the properties of such a system, but they all led to a dispersion relation with a minimum at non-zero wave vector. This behaviour is due to the specific form of the magnetic field and is not due to a mass mismatch.

To our knowledge there have been no calculations or experiments so far that show the above-mentioned peculiar behaviour as a result of a mass mismatch. Here we investigate the influence of several physical parameters, i.e. well depth, well width, magnetic field strength and mass ratio, on the behaviour of the dispersion relation. Furthermore, we investigate the expectation values of the potential and kinetic energy, in order to explain the peculiar behaviour.

This paper is organized as follows. In section 2 we derive the Schrödinger equation of our system, which is a quantum well with a magnetic field applied parallel to the interfaces and where a mass mismatch between the electrons in the barrier and in the well is included. We also indicate which numerical technique we have used to solve this differential equation. In section 3 we present our numerical results and study the dependence of the energy spectrum on the well width and height, the mass mismatch and the magnetic field strength. Our conclusions are presented in section 4.

2. Theoretical model

We consider a quantum well embedded in a barrier material with a magnetic field applied parallel to the surfaces of the well, taken to be the (x, y) plane, i.e. $\vec{B} = B_y \vec{e}_y$. The Hamiltonian then becomes

$$H = \frac{1}{2m}\left(\vec{p} + \frac{e}{c}\vec{A}\right)^2 + V(z)$$

where $V(z)$ is the electronic confinement potential. We choose the vector potential in the Landau gauge, $\vec{A} = (B_y z, 0, 0)$, which results in the Schrödinger equation

$$\left[\frac{1}{2m}(p_y^2 + p_z^2) + \frac{1}{2m}\left(p_x + \frac{e}{c}B_y z\right)^2 + V(z) - E\right]\psi(x, y, z) = 0. \tag{1}$$

Since p_y and p_z commute with H we can write

$$\psi(x, y, z) = \frac{1}{\sqrt{S}} e^{ik_x x} e^{ik_y y} \varphi_{n,k_x}(z) \tag{2}$$

and the Schrödinger equation becomes

$$\left[-\frac{\hbar^2}{2m} \frac{d^2}{dz^2} + \frac{1}{2m} \left(\hbar k_x + \frac{e}{c} B_y z \right)^2 + V(z) \right] \varphi_{n,k_x}(z) = \left(E + \frac{\hbar^2}{2m} k_y^2 \right) \varphi_{n,k_x}(z). \tag{3}$$

When we take into account the different masses for the electrons in each layer, i.e. $m = m(z)$, the above equation has to be modified into [9]

$$\left[-\frac{\hbar^2}{2} \frac{d}{dz} \frac{1}{m(z)} \frac{d}{dz} + \frac{1}{2m(z)} \left(\hbar k_x + \frac{e}{c} B_y z \right)^2 + V(z) \right] \varphi_{n,k_x}(z) = E_n(k_x, k_y) \varphi_{n,k_x}(z) \tag{4}$$

where the energy is $E_n(k_x, k_y) = E_n(k_x) + \hbar^2 k_y^2 / 2m^*$ and the mass is: $m(z) = m_b$ for $|z| > W/2$ (barrier); $m(z) = m_w$ for $|z| < W/2$ (well) and the potential is: $V(z) = V_0 = E_{c,\text{(barrier)}} - E_{c,\text{(well)}}$ for $|z| > W/2$ (barrier); $V(z) = 0$ for $|z| < W/2$ (well). We also define the mass ratio $\mu = m_b/m_w$, the electron effective mass $m^* = 1/\langle 1/\mu(z) \rangle$ (i.e. the average mass for electrons that can partially penetrate the barrier), the well width W and the conduction band energies in the barrier $E_{c,\text{(barrier)}}$ and in the well $E_{c,\text{(well)}}$. The magnetic length $l_B = \sqrt{\hbar c / e B_y}$ is used as the unit of length and $E_* = \hbar^2 / 2 m_w l_B^2 = \hbar \omega_c / 2$ (with $\omega_c = e B_y / m_w c$ the cyclotron frequency for an electron in the well region) as the unit of energy. The differential equation (4) can then be rewritten in a simpler form and the energy $E_n(k_x)$ can then be found by solving the following equation:

$$\left\{ -\frac{d}{dz} \frac{1}{\mu(z)} \frac{d}{dz} + \frac{(z + k_x)^2}{\mu(z)} + V(z) - E_n(k_x) \right\} \varphi_{n,k_x}(z) = 0. \tag{5}$$

Differential equation (5) was solved using different numerical techniques. In the first approach we solved the differential equation in the well and barrier separately. In the well the wave function consists of a linear combination of parabolic cylindrical functions (Weber functions), while in the barrier the wave function is a decaying function. By matching the function value φ_{n,k_x} and $\varphi'_{n,k_x}/m^*$ at the well edges we find the eigenenergies E. This method is very fast, and we found it to be accurate at high magnetic fields. Our second approach uses the finite-step discretization technique as described in reference [12]. The wave function is written as an N-dimensional vector and the differential equation is, within a finite-difference scheme, cast into the set of linear equations

$$\mathbf{A}\Phi = E\Phi \tag{6}$$

with $\mathbf{A}$ an $N \times N$ tridiagonal symmetric matrix and Φ a vector of length N. Using standard routines from the Eispack library we obtained the N lowest eigenvalues and eigenvectors. We found that this approach works for all magnetic fields. The disadvantage of this method is that it becomes slow if one requires high accuracy.

3. Numerical results

It is known that in parallel magnetic fields the dispersion relation $E(k_x)$ deviates from a parabolic form. In the presence of a magnetic field the energy at low k_x-values can no longer be described by a parabola: for k_x near zero it is more flattened than in the absence of a magnetic field. More surprising is that in the case of different masses for the carriers in the barrier and the well the minimum of the $E(k_x)$ curve is shifted to non-zero k_x. This can be clearly seen in figure 1, where we have plotted the dispersion relation for positive k_x-values (E is symmetric in k_x) for $\mu = 20$ (dotted curve) and $\mu = 1$, i.e. no mass mismatch (full curve).

In the inset of figure 1 we show the corresponding envelope functions at $k_x = 0$ and at the minimum $k_x = k_{\rm min}$. When compared to the zero-field solutions, the k_x-dependent eigenfunctions are modified by the magnetic field in two different ways: (i) the centre of the electron wave function $\langle z \rangle$ is shifted corresponding to [13]

$$\frac{\langle z \rangle_{n,k_x}}{l_B} = -k_x l_B + \frac{1}{2}\frac{{\rm d}E_n(k_x)/E_*}{{\rm d}k_x l_B} \tag{7}$$

and (ii) the width Δ of the states will change according to

$$\Delta^2_{n,k_x} = \langle z^2 \rangle_{n,k_x} - \langle z \rangle^2_{n,k_x}. \tag{8}$$

From the inset of figure 1 we notice that for large μ (dotted curve) the centre of mass of the wave function is shifted more away from the centre of the quantum well than for the case of equal masses (full curve). Furthermore, we see that the wave function is wider when there is a mass mismatch between barrier and well.

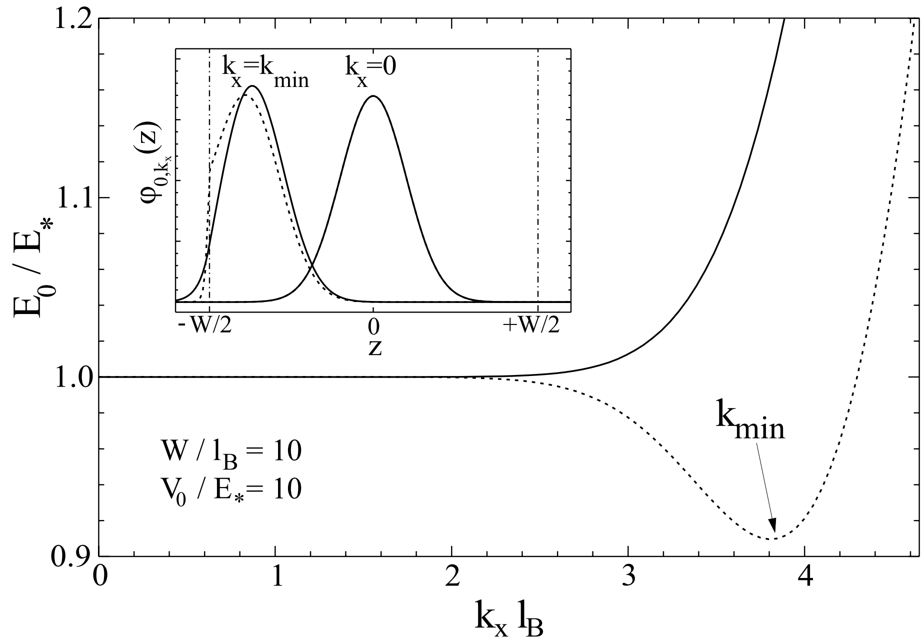

Figure 1. The energy dispersion relation $E_0(k_x)$ for the ground-state energy in the presence (dotted curve for $\mu = 20$) and in the absence (full curve) of a mass mismatch between electrons in the well and in the barrier. In the inset we show the electron wave function for $k_x = 0$ and $k_x = k_{\rm min}$, i.e. the wave vector where the dotted curve has its minimum. The dotted curve is for $\mu = 20$ and the full curve for $\mu = 1$.

This is made more visible in figure 2: the dashed curve gives the linear expression $-k_x l_B$ which is the average position of the electron in the absence of a confinement potential and the dotted (full) curve gives the calculated centre of mass for $\mu = 20$ ($\mu = 1$). For $k_x \to \infty$ the dotted and full curves would approach $\langle z \rangle_{0,k_x}/l_B = -\frac{1}{2}W/l_B = -5$ if the confinement were infinitely high. The dotted curve lies systematically lower than the full one which shows that in the case of a large mass ratio, the centre of the wave function is shifted more towards the barrier than in the case of equal masses. The lower inset of figure 2 shows that for increasing

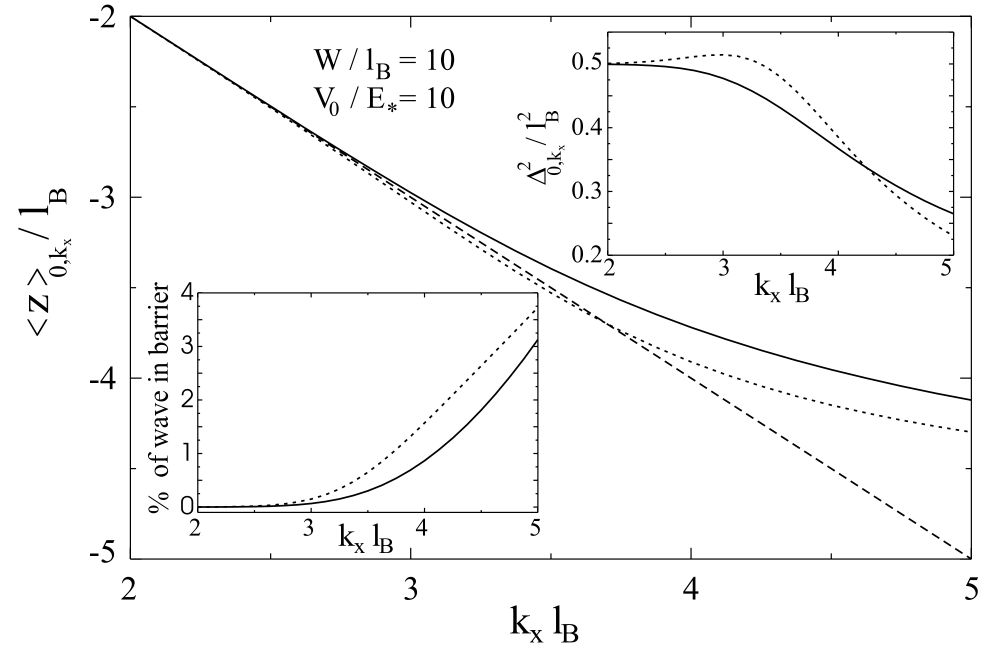

Figure 2. The average position of the electron as a function of the wave vector is shown in the absence of confinement (dashed curve) and for a quantum well with (dotted curve, $\mu = 20$) and without (full curve) mass mismatch. The dotted (full) curve of the lower inset gives the percentage of the wave function in the barrier for $\mu = 20$ ($\mu = 1$). The dotted (full) curve of the upper inset gives the width of the wave function for $\mu = 20$ ($\mu = 1$).

wave vector a larger percentage of the wave function is in the barrier when $\mu = 20$ (dotted curve) than when $\mu = 1$ (full curve). The upper inset of figure 2 shows the width of the wave function for increasing wave vector. For small k_x-values the dotted curve ($\mu = 20$) lies above the full one ($\mu = 1$), and we notice the peculiar behaviour of the width of the wave function: instead of being squeezed together, the wave function first becomes wider. For sufficiently large k_x-values the width decreases and for large k_x the wave function is narrower when μ is larger.

We found also a striking well width dependence. In figure 3 we show the ground-state energy at zero wave vector, i.e. $E_0(k_x = 0, k_y = 0)$, as a function of the well width for a fixed magnetic field and a mass ratio of $\mu = 1$ (full curve) and $\mu = 20$ (dotted curve). For large well widths ($>7\ W/l_B$) the $k_x = 0$ state is centred in the middle of the well and the confinement results predominantly from the magnetic field since the envelope function does not 'feel' the barrier and consequently there is no μ-dependence. When we decrease the well width the wave function starts entering the barrier and we expect the energy to increase. The dotted curve shows instead the opposite behaviour: decreasing the well width decreases the energy. This effect is a consequence of the mass mismatch as can be seen from the full curve in figure 3 where the mass mismatch is completely neglected and which shows that the energy always increases with decreasing well width. A similar behaviour is seen for the energy minimum, i.e. $E_0(k_x = k_{\min}, k_y = 0)$ (dashed curve) when $\mu = 20$. A contour plot of the energy of the $n = 0$ state in $\boldsymbol{k}$-space for $\mu = 20$, $W/l_B = 8$ and $V_0/E_* = 10$ is shown in the inset of figure 3. The two local minima are clearly visible.

To investigate this special feature in more detail we look at its dependence on different

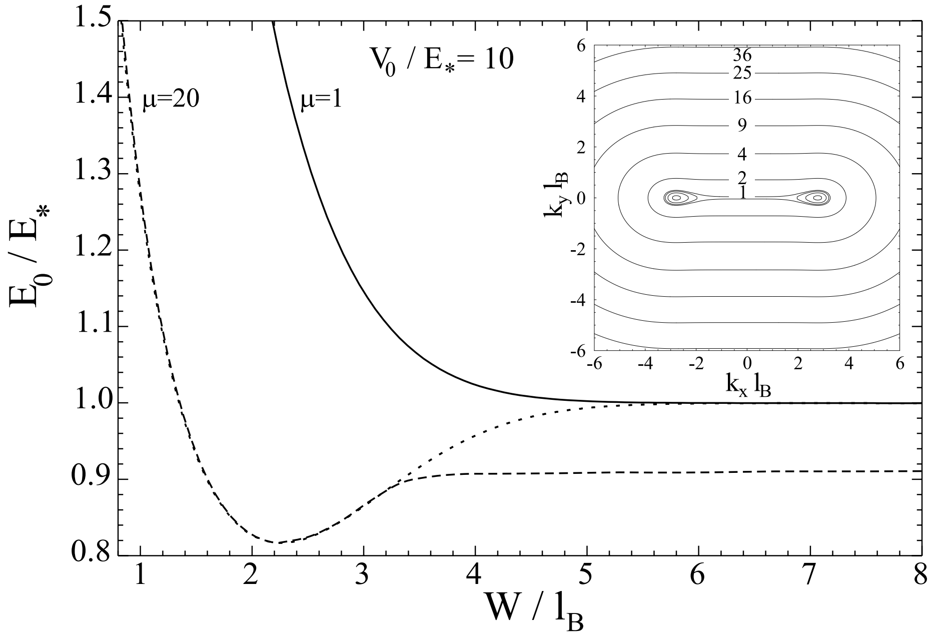

Figure 3. The energy at zero wave vector, i.e. $E_0(k_x = 0)$, as a function of the well width for $\mu = 20$ (dotted curve) and $\mu = 1$ (full curve) and at $k_x = k_{\min}$ (dashed curve) for $\mu = 20$. The inset shows a contour plot of the energy of the lowest state for $\mu = 20$, i.e. $E_0(k_x, k_y)$

important parameters: B_y (magnetic field), V_0 (well depth) and μ (mass ratio). To show the effect of changing the magnetic field B_y, the ground-state dispersion curves $E_0(k_x)$ are plotted in figure 4 for different values of the magnetic field. Changing the magnetic field will change the unit of length l_B and the unit of energy E_* and therefore we have taken an InAs/GaSb quantum well system with a well width of 40 nm, a well height of 950 meV and a mass ratio of $\mu = m_{\mathrm{GaSb}}/m_{\mathrm{InAs}} = 0.047/0.023 = 2.04$. We notice that increasing the magnetic field increases the effect of having the minimum at $k_x \neq 0$. At $B_y = 1$ T the dispersion curve has its minimum at $k_x = 0$, but for $B = 20$ T it clearly has a minimum at k_x different from 0. Somewhere between these two values the behaviour of the dispersion curve changes drastically. In the inset of figure 4 we show the $k_{\min}$-value where the ground-state ($n = 0$) and first-excited-state ($n = 1$) energies $E_n(k_{\min})$ attain their minimum values. Notice that there is a threshold value (7 T for the ground state and 9.75 T for the excited state) for which the special behaviour in the energy starts to appear. For values under this threshold value the minimum is at $k_x = 0$, for values above the threshold value the minimal k_x-value increases abruptly and for higher magnetic fields it continues to increases linearly, i.e. $k_{\min} = a(B_y - b)$, with a a scaling factor and b the extrapolated threshold value for the magnetic field which we find if we extrapolate this linear behaviour to $k_{\min} = 0$ (see the thin line in the inset of figure 4). For the ground state we found $a = 0.025$ nm^{-1} T^{-1} and $b = 5.88$ T and for the first excited state $a = 0.023$ nm^{-1} T^{-1} and $b = 8.34$ T.

Figure 5 shows the effect of changing the well depth V_0. We notice again that there exists a threshold value between $V_0/E_* = 0$ and 1.5 for the well depth that must be reached before the energy shows a local minimum at $k_x \neq 0$. For well depths under this value, there exists no local minimum; the dispersion decreases monotonically. This is due to the fact that for such low values of the well depth, the wave function is pushed outside the well for increasing k_x-value.

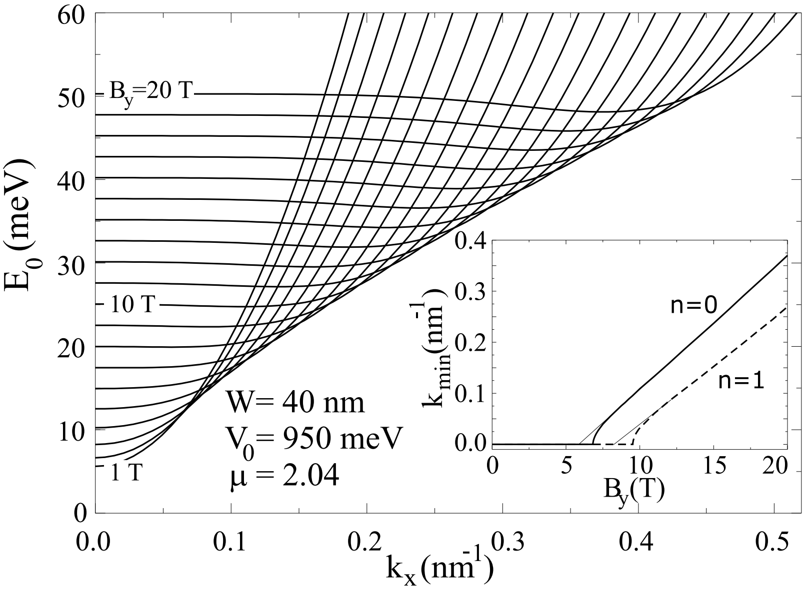

Figure 4. The dispersion curves $E_0(k_x)$ for the ground state for different magnetic fields varying from $B = 1$ T to $B = 20$ T in steps of 1 T. The inset shows the value of the wave vector where the minimum in the energy dispersion relation occurs, i.e. k_{min}, as a function of the magnetic field for the two lowest energy levels, i.e. $n = 0$ and $n = 1$. The thin lines are the linear fits to which these curves converge at high magnetic fields.

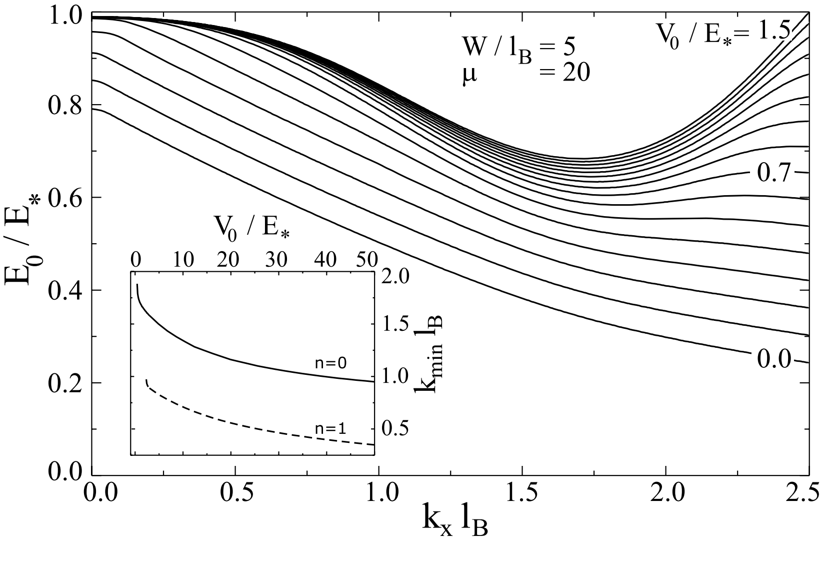

Figure 5. The dispersion curves for the ground state for different well depths varying from $V_0/E_* = 0.0$ to $V_0/E_* = 1.5$ in steps of 0.1. In the inset we show k_{min} versus V_0/E_* for the two lowest energy levels.

For large enough wave vectors, the wave function is confined by the magnetic confinement and does not 'feel' the electronic confinement. In the inset we show the k_{min}-value at which the energy $E_n(k_{\mathrm{min}})$ attains its minimum value for $n = 0$ (ground state) and $n = 1$ (first excited state). For well depths between 0 and 0.7 (0 and 2) there exists no local minimum in the ground-state (first-excited-state) energy while for deeper wells the local minimum is moved to lower k_x-values.

Figure 6 shows the effect of changing the mass ratio between the barrier and the well. As expected, the effect of having $k_{\min} \neq 0$ becomes larger when the mass in the barrier becomes larger than in the well. From the inset we notice again that there exists a certain threshold mass ratio that must be reached for the effect to appear. For a mass ratio under this threshold the minimum is at $k_{\min} = 0$; for larger mass mismatches the minimal k_x-value increases faster than a simple power law, but we were able to fit it to the following expression:

$$k_{\min} = a \exp\left(\frac{-c}{\mu - b}\right)$$

with $a = 1.48$ (0.77) l_B^{-1} a scaling factor, $b = 1.17$ (1.71) the threshold value for the mass ratio and $c = 1.23$ (2.60) for the ground state (first excited state).

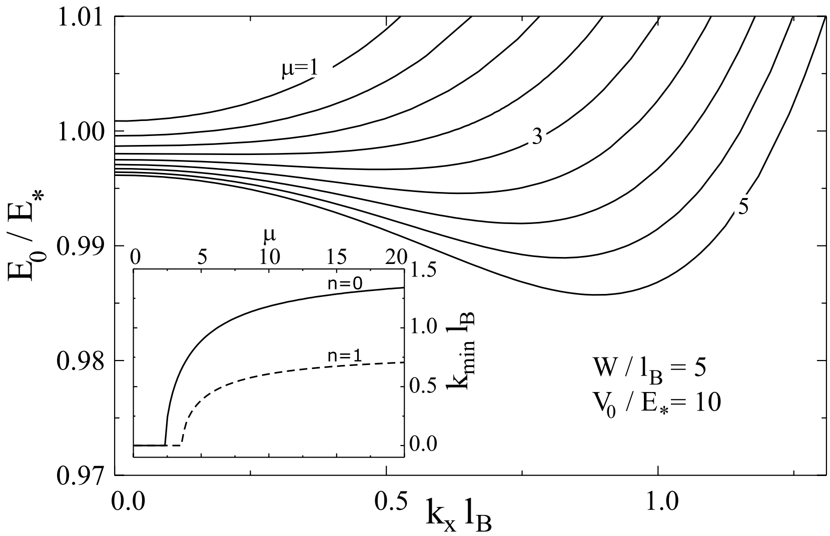

Figure 6. The dispersion curves for the ground state for different mass ratio varying from $\mu = 1$ to $\mu = 5$ in steps of 0.5. In the inset we plotted $k_{\min}$ versus μ for the two lowest levels.

In order to find the physical origin of the local minimum in the dispersion relation we investigated the behaviour of the different terms in the Hamiltonian. From equation (5) we know that the system is described by the following Hamiltonian:

$$H = -\frac{\mathrm{d}}{\mathrm{d}z}\frac{1}{\mu(z)}\frac{\mathrm{d}}{\mathrm{d}z} + \frac{(z+k_x)^2}{\mu(z)} + V(z) \qquad (9)$$

and we will calculate the expectation values of each of the different terms in the Hamiltonian. In figure 7 we plotted these three terms together with the total ground-state energy (full curve) and compare the situation with (a) and without (b) mass mismatch at the well–barrier interface. The dotted curve represents

$$\left\langle -\frac{\mathrm{d}}{\mathrm{d}z}\frac{1}{\mu(z)}\frac{\mathrm{d}}{\mathrm{d}z}\right\rangle$$

which is the kinetic energy, the dashed curve represents $\langle (z+k_x)^2/\mu(z)\rangle$, the magnetic energy, and the dash–dotted line gives $\langle V(z)\rangle$, the contribution due to the barrier potential. From figure 7(a) ($\mu = 1$) we notice that the total energy (full curve) is mainly composed of the kinetic and magnetic energy, and although we have a local minimum in the magnetic term at $k_x l_B = 3.7$, this does not result in a local minimum in the total energy. In the case of a mass mismatch (figure 7(b) ($\mu = 20$)) the kinetic term (dashed curve) is substantially lower and exhibits a local minimum at $k_x l_B = 3.6$ and the local minimum in the magnetic energy (dotted curve) is much more pronounced and is shifted to a larger k_x-value, i.e. $k_x l_B = 4.2$. The combined effect of these two terms leads to a local minimum in the total energy which appears at $k_x l_B = 3.7$ which is between the positions of the local minima in the kinetic and magnetic energy.

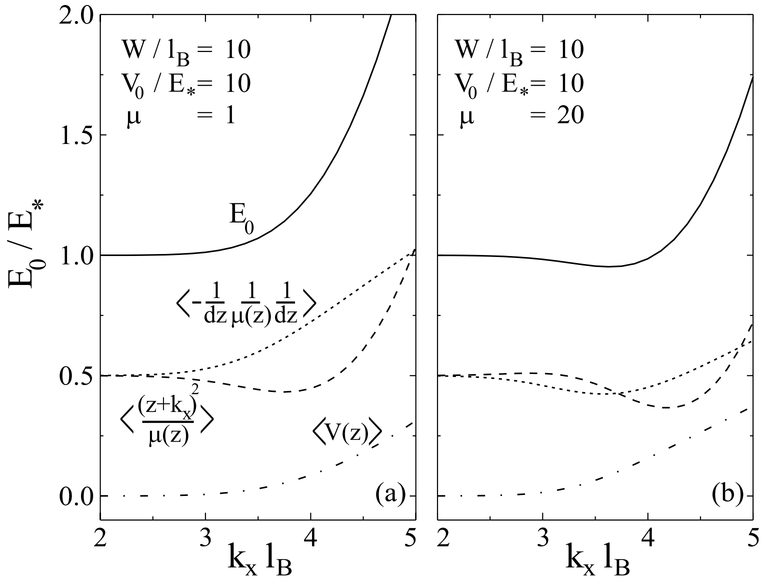

Figure 7. The expectation values of the different terms in the Hamiltonian (see equation (9)): the total energy $E_0(k_x)$ (full curve), the kinetic energy term $\langle(-\mathrm{d}/\mathrm{d}z)(1/\mu(z))\,\mathrm{d}/\mathrm{d}z\rangle$ (dashed curve), the magnetic energy term $\langle(z + k_x)^2/\mu(z)\rangle$ (dotted curve) and the potential energy $\langle V(z)\rangle$ (dash–dotted curve). We show the result (a) without mass mismatch ($\mu = 1$) and (b) with a large mass mismatch ($\mu = 20$).

A simple physical picture can be given by noting that in the case of a mass mismatch, for larger k_x-values, electrons can penetrate more into the barrier (see the lower inset of figure 2) where the electron mass is larger. As a consequence the potential energy will increase slightly (see the dash–dotted curve in figure 7), but this is not enough to offset the decrease in the kinetic and magnetic energy terms.

4. Conclusions

We investigated the system consisting of a quantum well, with a magnetic field applied in the plane of the well layers. We have included the effect of mass mismatch between the barrier and the well and found that this gives rise to a minimum in the dispersion relation $E_n(k_x)$ at non-zero wave vector. We have looked at the influence of several physical parameters, i.e. magnetic field, well width, well depth and mass ratio, on the behaviour of the dispersion relation. We observed that in an InAs/GaSb quantum well of width 40 nm, where the mass of the electrons in the barrier is about twice the mass of the electrons in the well, the minimum in the dispersion relation occurs at a magnetic field of 7 T. To explain the peculiar behaviour we have calculated the expectation values of the kinetic and potential energy, and found that the effect is mainly due to a larger penetration of the wave function into the barrier which decreases the kinetic and magnetic energy terms in the Hamiltonian.

Acknowledgments

This work was partially supported by the Inter-university Micro-Electronics Centre (IMEC, Leuven), the Flemish Science Foundation (FWO-Vl) and the IUAP-IV. RDM is supported by 'het Vlaams Instituut voor de bevordering van het Wetenschappelijk & Technologisch Onderzoek in de Industrie' (IWT) and FMP is a research director of the Fund for Scientific Research, Flanders, Belgium (FWO).

References

[1] Stern F and Howart W 1967 *Phys. Rev.* **163** 816
[2] Smrčka L and Jungwirth T 1994 *J. Phys.: Condens. Matter* **6** 55
[3] Smrčka L and Jungwirth T 1995 *J. Phys.: Condens. Matter* **7** 3721
[4] Lakrimi M, Khym S, Nicholas R, Symons D, Peeters F, Mason N and Walker P J 1997 *Phys. Rev. Lett.* **79** 3034
[5] Gauer C, Wixforth A, Kotthaus J, Abstreiter G, Weimann G and Schlapp W 1995 *Europhys. Lett.* **30** 111
[6] Hu J and MacDonald A 1992 *Phys. Rev.* B **46** 12 554
[7] Tang H and Butcher P 1988 *J. Phys. C: Solid State Phys.* **21** 3959
[8] Heisz J and Zaremba E 1993 *Semicond. Sci. Technol.* **8** 575
[9] Bastard G 1988 *Wave Mechanics applied to Semiconductor Heterostructures* (Les Ulis: Les Éditions de Physique) pp 74–6
[10] Rashba E I 1959 *Sov. Phys.–Solid State* **1** 368
[11] Ibrahim I and Peeters F 1995 *Phys. Rev.* B **52** 17 321
[12] MacKeown P K and Newman D J 1987 *Computational Techniques in Physics* (Bristol: Hilger) pp 51–73
[13] Jungwirth T and Smrčka L 1993 *Superlatt. Microstruct.* **13** 499